Electronic Supplementary Material (ESI) for RSC Advances.

Supporting Information
Electronic structure, low-temperature transport and thermodynamic properties of polymorphic $\beta-As_2Te_3$

J.-B. Vaney[1], J.-C. Crivello[2], C. Morin[2], G. Delaizir[3], J. Carreaud[3], A. Piarristeguy[4], J. Monnier[2], E. Alleno[2], A. Pradel[4], E. B. Lopes[5], A. P. Gonçalves[5], A. Dauscher[1], C. Candolfi[1], and B. Lenoir*[1]

[1]Institut Jean Lamour, UMR 7198 CNRS – Université de Lorraine, Nancy, France

[2]Institut de Chimie et des Matériaux Paris Est (ICMPE), UMR 7182 CNRS-Université Paris-Est Créteil, Thiais, France

[3]Science des Procédés Céramiques et de Traitements de Surface (SPCTS), UMR CNRS 7315-Université de Limoges, France

[4]Institut Charles Gerhardt (ICG), UMR 5253 CNRS-Université de Montpellier, France

[5]C2TN, Instituto Superior Técnico, Universidade de Lisboa, Lisboa, Portugal

*Corresponding author: bertrand.lenoir@univ-lorraine.fr

Contents

1 Rietveld refinements of the PXRD pattern of $\beta-As_2Te_3$

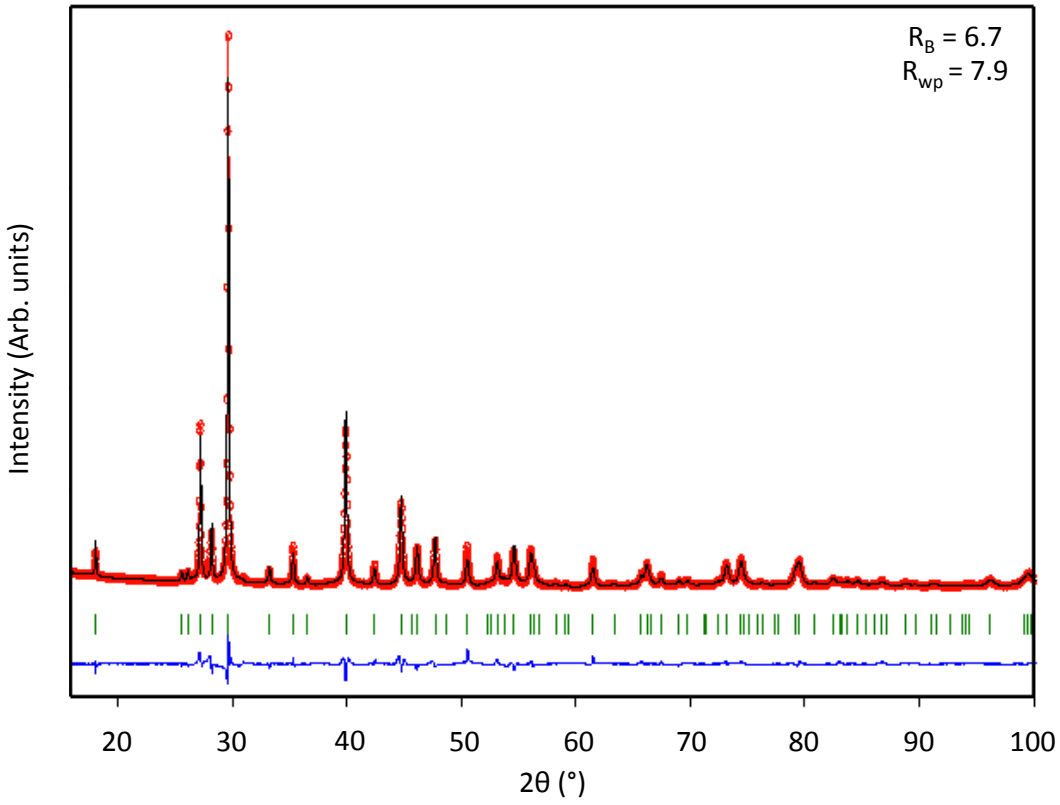

Figure S1: Experimental PXRD pattern of $\beta-As_2Te_3$ and its Rietveld analysis. The red open circles are the experimental data, the black line is the calculated pattern, the bottom blue line is the difference between the experimental and calculated pattern and the green vertical ticks stand for the Bragg reflections of $\beta-As_2Te_3$.

2 DFT results on As_2Te_3: α, β, β' phases

2.1 Crystal structures

2.1.1 Summary of the studied phases

	α	β	β'	β'
	$C2/m$ (12)	$R\bar{3}m$ (166)	$C2/m$ (12)	$P2_1/m$ (11)
a (Å)	14.962	4.102	7.088	7.087
b/a	0.272	1	0.577	2.309
c/a	1.152	7.173	1.476	1.478
β	95.576	*hex*	103.044	103.016
volume (Å^3/at)	30.701	28.893	29.560	29.592

The following crystal structures are given in the POSCAR format, as an input file for VASP code (see: http://cms.mpi.univie.ac.at/vasp/guide/node59.html).

2.1.2 $\alpha-As_2Te_3$ phase, $C2/m(12)$

```
Alpha C2/m (12)
   1.00000000000000
    14.8909628327804597    0.0000000000000000   -1.4546505915510886
     0.0000000000000000    4.0707151357359228    0.0000000000000000
     0.0001027857736047    0.0000000000000000   10.1295988835578967
   Te   As
    12    8
Direct
  0.0416753433619590  0.0000000000000000  0.2877346020687099 # Te1 (4i)
  0.9583246566380694  0.0000000000000000  0.7122653979314180
  0.2179249110261594  0.0000000000000000  0.6642957363094482
  0.7820750889738690  0.0000000000000000  0.3357042636906158
  0.2820750889738406  0.5000000000000000  0.3357042636906158 # Te2 (4i)
  0.1298277017099139  0.5000000000000000  0.9691725449397950
  0.8701722982900932  0.5000000000000000  0.0308274550601411
  0.4583246566380552  0.5000000000000000  0.7122653979314180
  0.3701722982900577  0.0000000000000000  0.0308274550601411 # Te3 (4i)
  0.5416753433619306  0.5000000000000000  0.2877346020687099
  0.7179249110261310  0.5000000000000000  0.6642957363094482
  0.6298277017099068  0.0000000000000000  0.9691725449397950
  0.1248755341288188  0.5000000000000000  0.4396573642955062 # As1 (4i)
  0.8751244658711457  0.5000000000000000  0.5603426357044299
  0.7947309319160141  0.0000000000000000  0.8590069449202105
  0.3751244658711244  0.0000000000000000  0.5603426357044299
  0.2052690680839433  0.0000000000000000  0.1409930550798109 # As2 (4i)
  0.6248755341288543  0.0000000000000000  0.4396573642955062
  0.2947309319160425  0.5000000000000000  0.8590069449202105
  0.7052690680839859  0.5000000000000000  0.1409930550798109
```

2.1.3 $\beta-\mathbf{As_2Te_3}$ phase, $R\bar{3}m(166)$

```
beta R-3m (166) - hexagonal description
     1.00000000000000
     4.1017556079257629   -0.0000000000000127   -0.0000000000000001
    -2.0508778039629871    3.5522245565756223   -0.0000000000000001
     0.0000000000000010    0.0000000000000012   29.7451589947873316
   Te   As
     9     6
Direct
  0.0000000000000000  0.0000000000000000  0.2176841539434236 # Te1 (6c)
  0.6666666666666643  0.3333333333333357  0.1156491793899264
  0.3333333333333357  0.6666666666666643  0.8843508206099742
  0.3333333333333357  0.6666666666666643  0.4489825127232407
  0.0000000000000000  0.0000000000000000  0.7823158460566901
  0.6666666666666643  0.3333333333333357  0.5510174872766456
  0.0000000000000000  0.0000000000000000  0.0000000000000000 # Te2 (3a)
  0.3333333333333357  0.6666666666666643  0.6666666666666643
  0.6666666666666643  0.3333333333333357  0.3333333333333357
  0.6666666666666643  0.3333333333333357  0.9379151253680860 # As (6c)
  0.3333333333333357  0.6666666666666643  0.0620848746319069
  0.3333333333333357  0.6666666666666643  0.2712484587013932
  0.0000000000000000  0.0000000000000000  0.3954182079652711
  0.0000000000000000  0.0000000000000000  0.6045817920347503
  0.6666666666666643  0.3333333333333357  0.7287515412985854
```

2.1.4 $\beta'-\mathbf{As_2Te_3}$ phase, $C2/m(12)$

```
Beta-prime C2/m (12)
   1.00000000000000
     6.9046540434222221    0.0000000000000000   -1.5996322569318127
     0.0000000000000000    4.0917922360543972    0.0000000000000000
    -0.0000156673416340    0.0000000000000000   10.4627509324877295
   Te   As
     6     4
Direct
  0.0000000000000000  0.0000000000000000  0.0000000000000000 # Te1 (2a)
  0.5000000000000000  0.5000000000000000  0.0000000000000000
  0.2204183099257193  0.0000000000000000  0.6610508751331210 # Te2 (4i)
  0.7795816900742807  0.0000000000000000  0.3389491248668790
  0.7204183099257193  0.5000000000000000  0.6610508751331210
  0.2795816900742807  0.5000000000000000  0.3389491248668790
  0.8940851239894982  0.5000000000000000  0.1823290164472340 # As (4i)
  0.1059148760105018  0.5000000000000000  0.8176709835527660
  0.3940851239894982  0.0000000000000000  0.1823290164472340
  0.6059148760105018  0.0000000000000000  0.8176709835527660
```

2.1.5 $\beta'-\mathbf{As_2Te_3}$ phase, $P2_1/m(11)$

```
Beta-prime-bis P2_1/m (11)
   1.0
     6.9045518024777408    0.0000000000000000   -1.5970740485871309
     0.0000000000000000   16.3655751398697511    0.0000000000000000
     0.0000000000000000    0.0000000000000000   10.4751313887324446
  24  16
Direct
  0.0000000000000000  0.0000000000000000  0.0000000000000000 # Te1 (2a)
  0.0000000000000000  0.5000000000000000  0.0000000000000000
  0.0000013036320369  0.2500000000000000  0.0000012660758330 # Te2 (2e)
  0.9999986963679631  0.7500000000000000  0.9999987339241670
  0.5000009464446676  0.1249999942479898  0.0000004059690083 # Te3 (4f)
  0.4999990535553324  0.8750000057520102  0.9999995940309917
  0.4999990535553324  0.6249999942479898  0.9999995940309917
  0.5000009464446676  0.3750000057520103  0.0000004059690083
  0.2205914831849745  0.0000000151540891  0.6614859450879841 # Te4 (4f)
  0.7794085168150255  0.9999999848459109  0.3385140549120159
  0.7794085168150255  0.5000000151540891  0.3385140549120159
  0.2205914831849745  0.4999999848459109  0.6614859450879841
  0.2205932961392882  0.2500000000000000  0.6614857889388425 # Te5 (2e)
  0.7794067038607118  0.7500000000000000  0.3385142110611575
  0.2205896412270864  0.7500000000000000  0.6614858772079598 # Te6 (2e)
  0.7794103587729135  0.2500000000000000  0.3385141227920402
  0.7205926019527990  0.1249998811078998  0.6614859142170191 # Te7 (4f)
  0.2794073980472010  0.8750001188921002  0.3385140857829809
  0.2794073980472010  0.6249998811078998  0.3385140857829809
  0.7205926019527990  0.3750001188921002  0.6614859142170191
  0.7205903500590526  0.6250000715243422  0.6614858650711092 # Te8 (4f)
  0.2794096499409474  0.3749999284756577  0.3385141349288908
  0.2794096499409474  0.1250000715243423  0.3385141349288908
  0.7205903500590526  0.8749999284756578  0.6614858650711092
  0.3939978591268419  0.2500000000000000  0.1821117369113082 # As1 (2a)
  0.6060021408731581  0.7500000000000000  0.8178882630886919
  0.3939948955795695  0.7500000000000000  0.1821121029395504 # As2 (2e)
  0.6060051044204304  0.2500000000000000  0.8178878970604496
  0.3939965854323068  0.4999996220338493  0.1821113836346699 # As3 (4f)
  0.6060034145676931  0.5000003779661506  0.8178886163653301
  0.6060034145676931  0.9999996220338494  0.8178886163653301
  0.3939965854323068  0.0000003779661507  0.1821113836346699
  0.1060047195806245  0.1249993893488116  0.8178873164696396 # As4 (4f)
  0.8939952804193755  0.8750006106511885  0.1821126835303604
  0.8939952804193755  0.6249993893488115  0.1821126835303604
  0.1060047195806245  0.3750006106511884  0.8178873164696396
  0.1060023179201455  0.6250006367550300  0.8178893759312342 # As5 (4f)
  0.8939976820798545  0.3749993632449700  0.1821106240687658
  0.8939976820798545  0.1250006367550300  0.1821106240687658
  0.1060023179201455  0.8749993632449700  0.8178893759312342
```

2.2 Electronic structures

Reading help

For each structure, the total DOS are presented on top of each phase-section, followed by the partial contribution on each inequivalent site: Te on left, As on right.

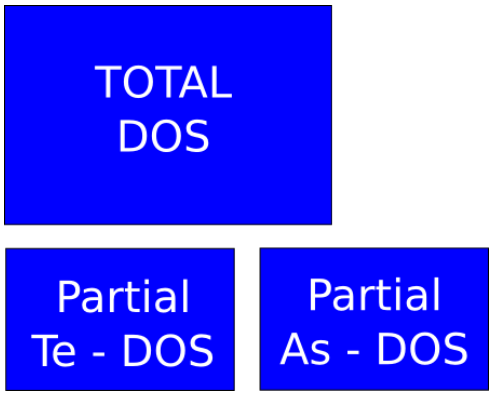

The total DOS is represented (red line, left scale) with the number of valence electrons (dashed green line, right scale). Values are given for the primitive cell formula: 20, 15, 10 and 40 atoms for α, β, $\beta' - C2/m$, and $\beta' - P2_1/m$, respectively.
The partial DOS presents the contribution on each orbital: s electrons ($l = 0$) is in blue, p ($l = 1$) in green and d ($l = 2$) in red.
The Fermi level is shifted to the origin of energy.

2.2.1 $\alpha-\mathbf{As_2Te_3}$ phase, $C2/m(12)$

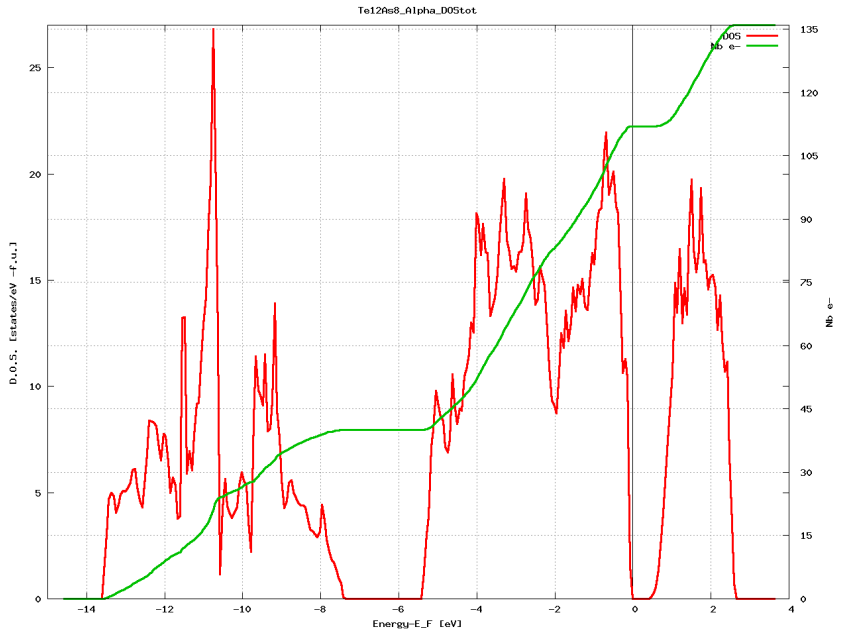

Figure S2: Total DOS of $\alpha-As_2Te_3$ phase.

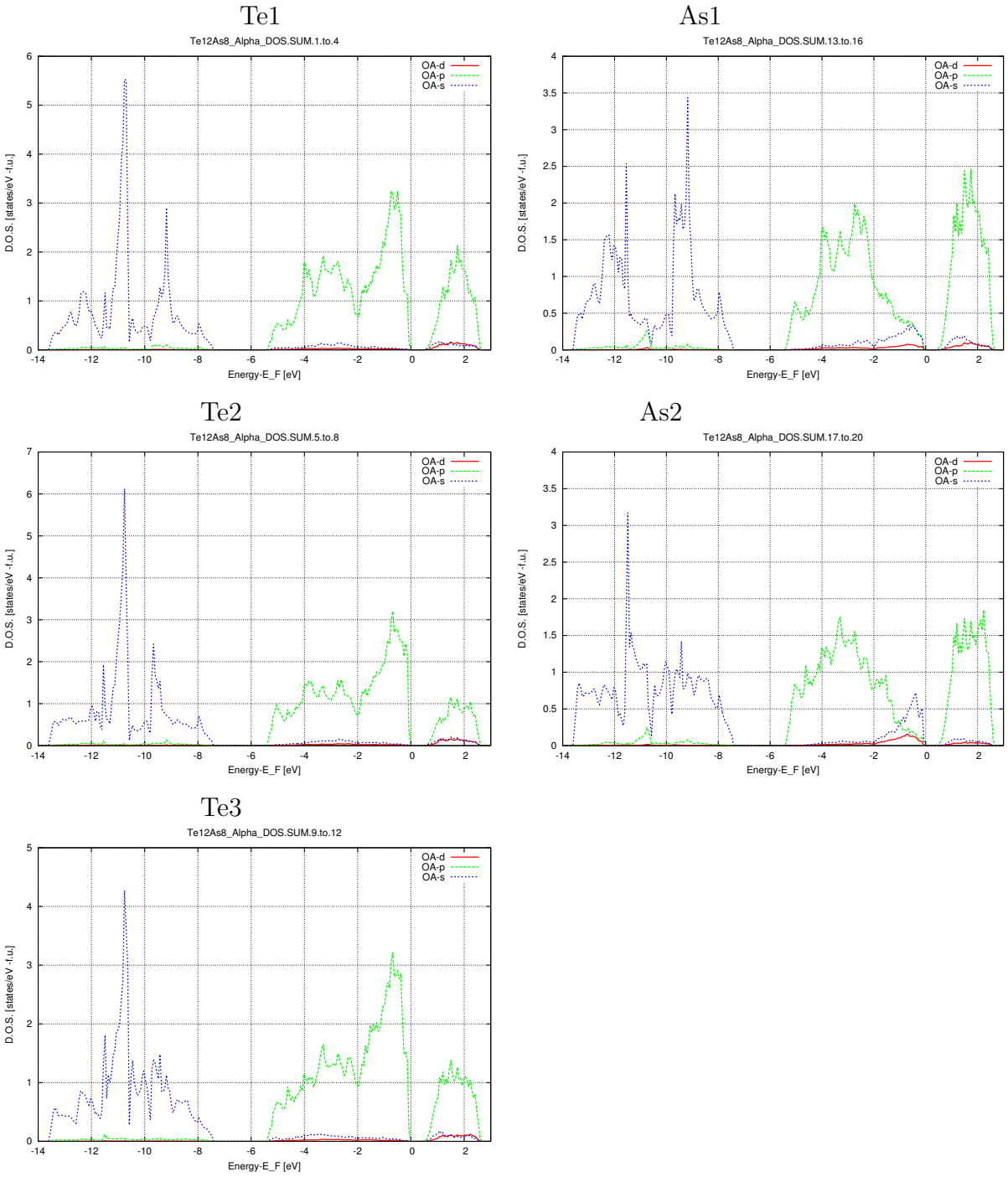

Figure S3: Partial DOS of $\alpha-As_2Te_3$ phase.

2.2.2 $\beta-As_2Te_3$ phase, $R\bar{3}m(166)$

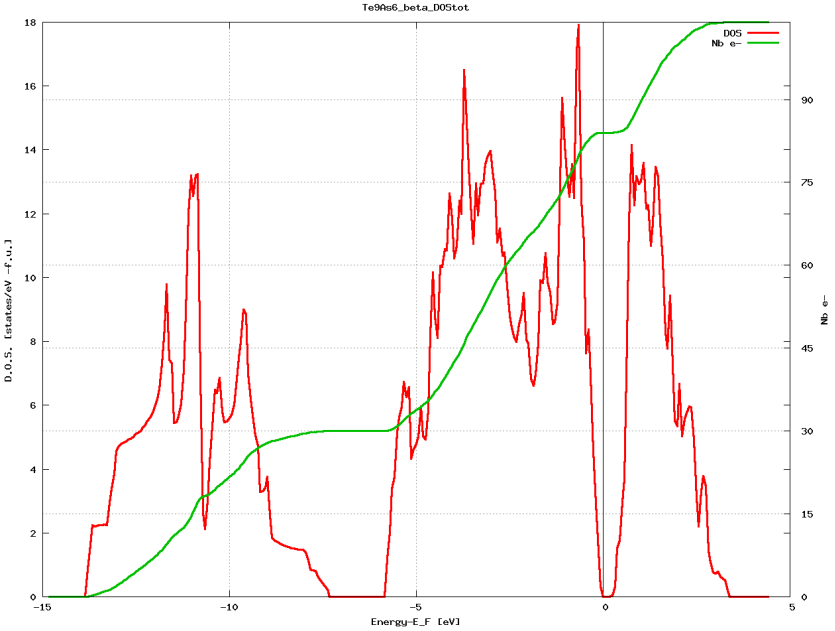

Figure S4: Total DOS of $\beta-As_2Te_3$ phase.

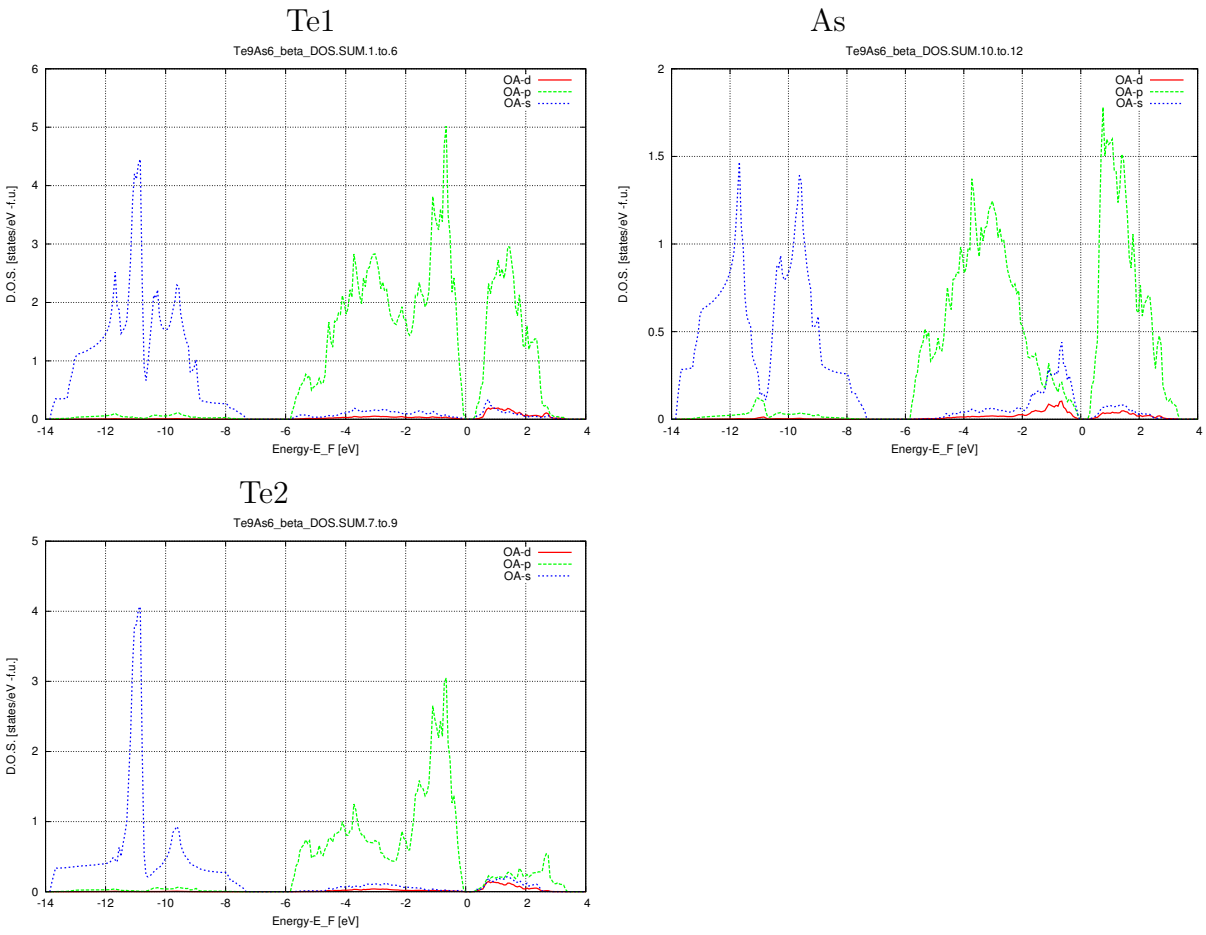

Figure S5: Partial DOS of $\beta-As_2Te_3$ phase.

2.2.3 $\beta'-\mathbf{As_2Te_3}$ phase, $C2/m(12)$

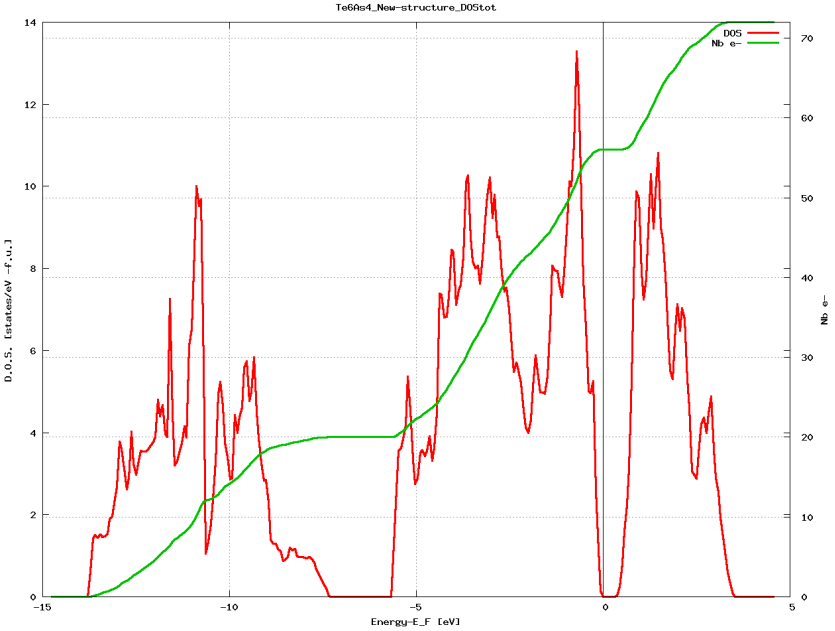

Figure S6: Total DOS of $\beta'-As_2Te_3$ phase, $C2/m(12)$.

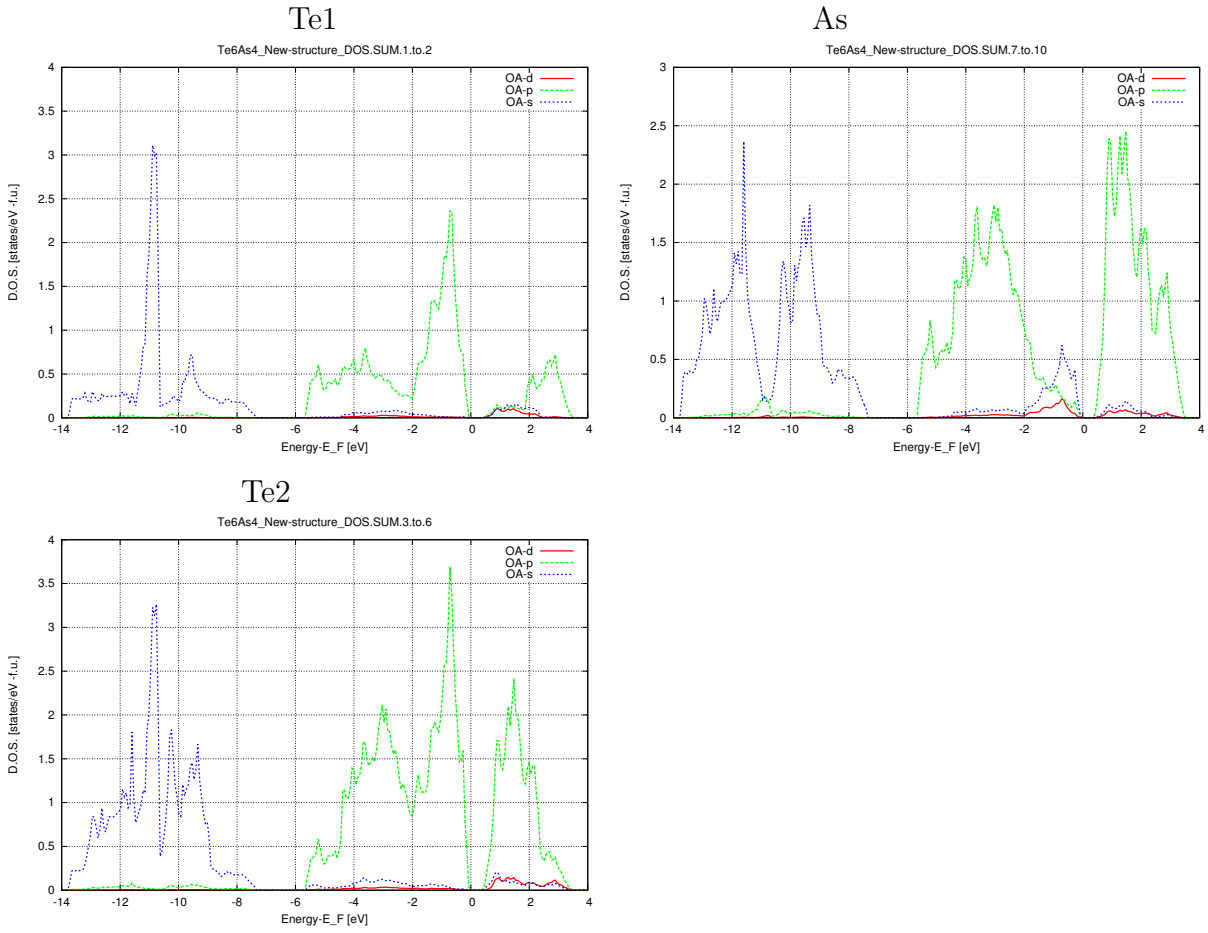

Figure S7: Partial DOS of $\beta'-As_2Te_3$ phase, $C2/m(12)$.

2.2.4 $\beta'-\mathbf{As_2Te_3}$ phase, $P2_1/m(11)$

Figure S8: Total DOS of $\beta'-\mathrm{As_2Te_3}$ phase, $P2_1/m(11)$.

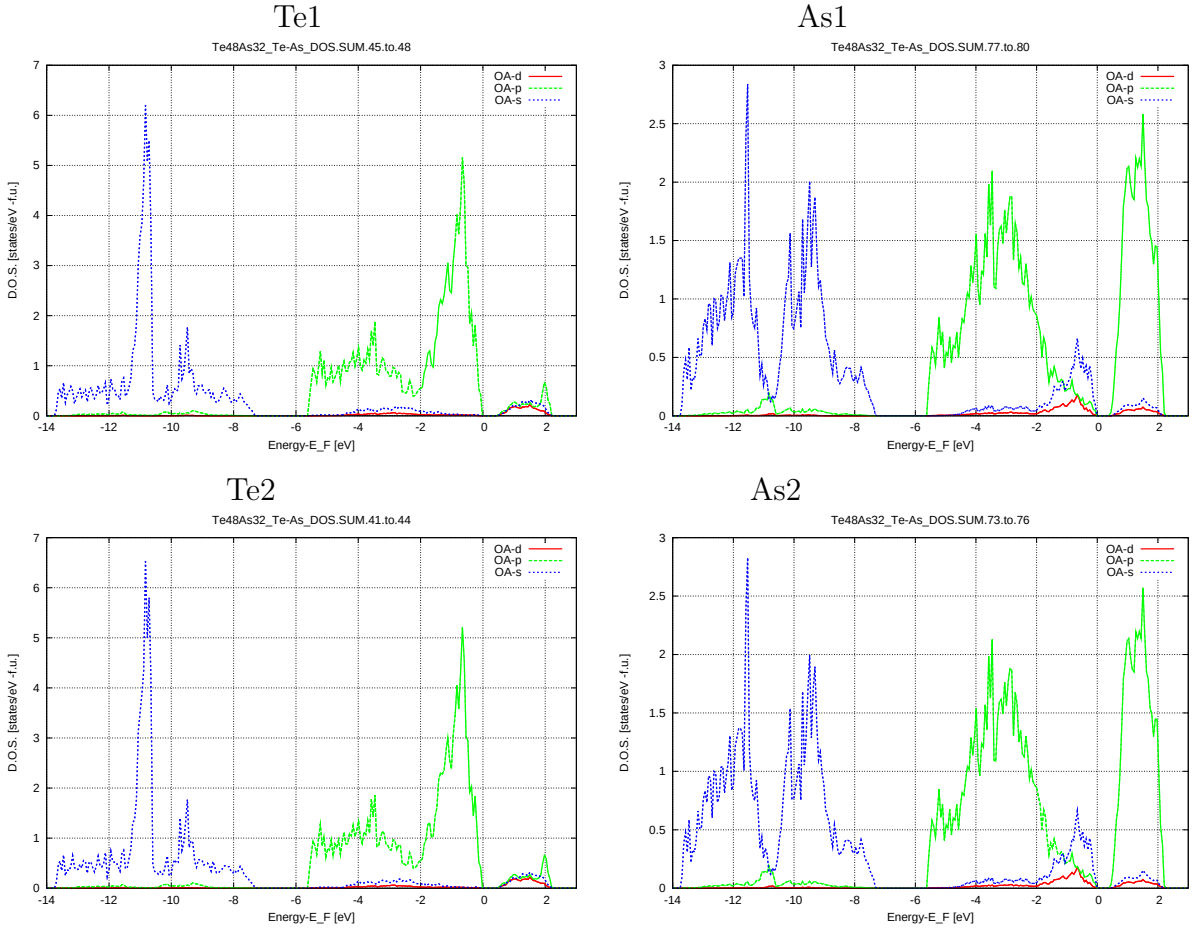

Te3

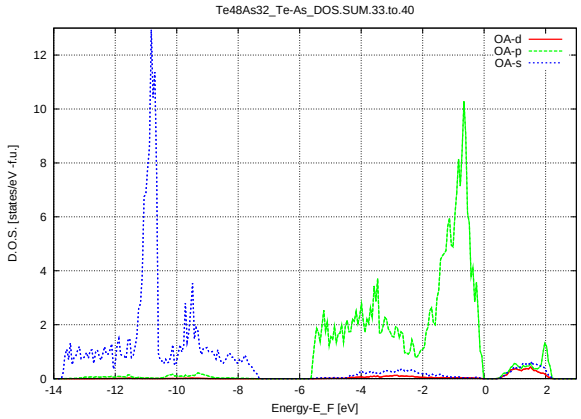

As3

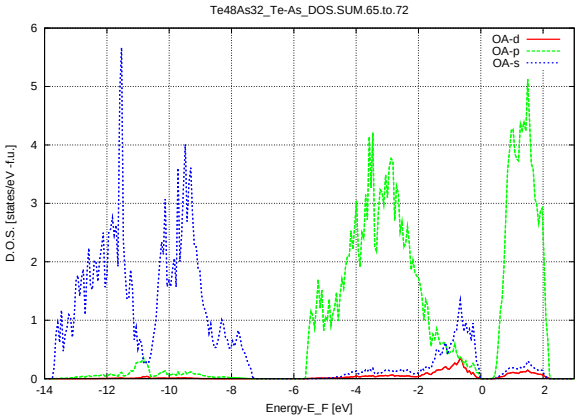

Te4

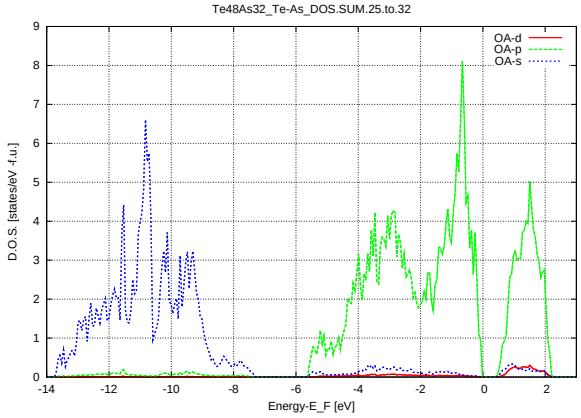

As4

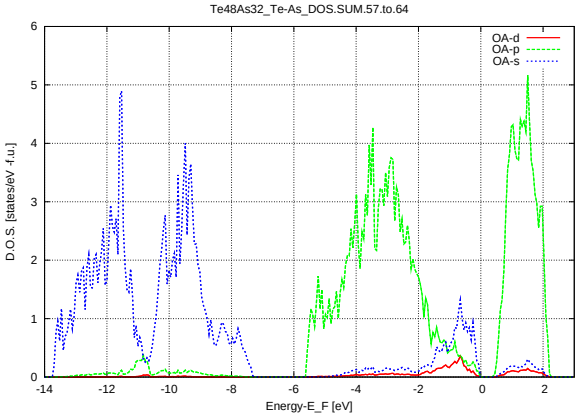

Te5

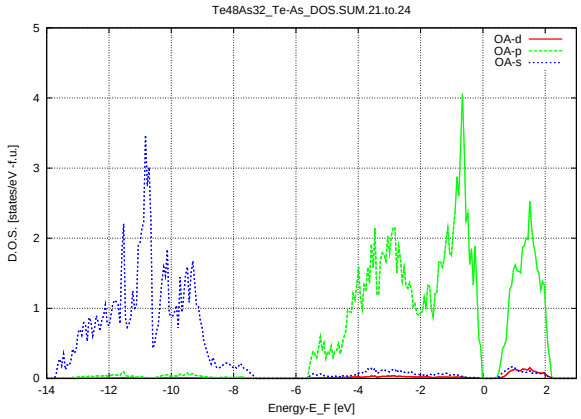

As5

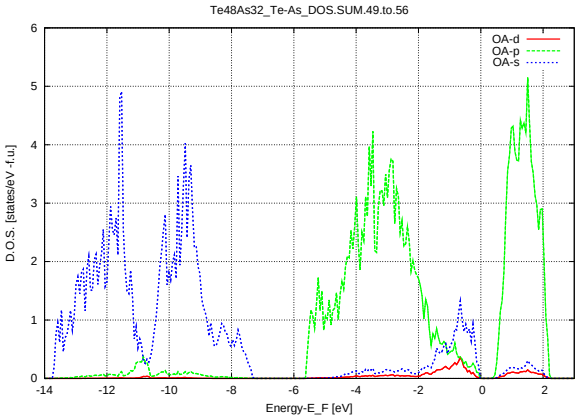

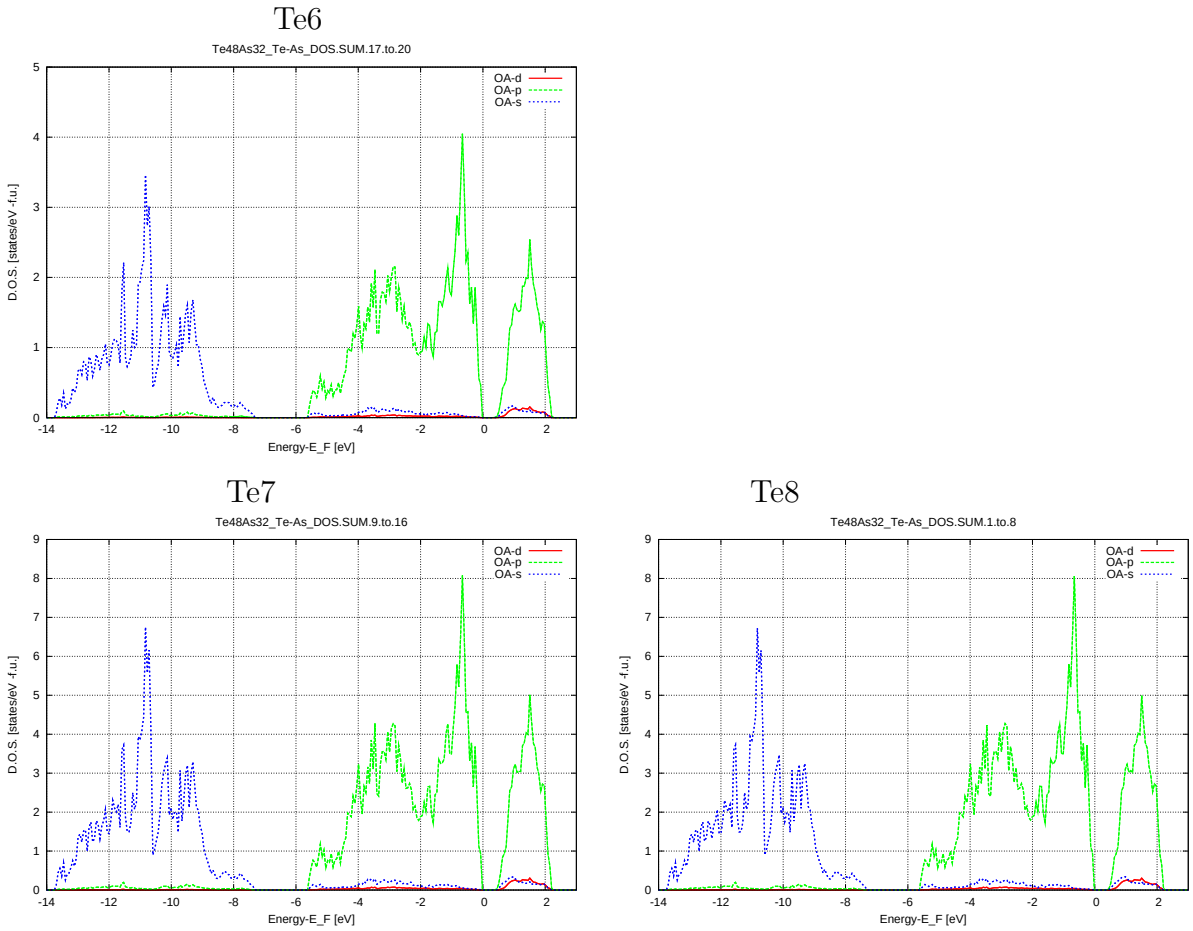

Figure S9: Partial DOS of $\beta'-As_2Te_3$ phase, $P2_1/m(11)$.

2.3 Vibrational properties

The following results has been obtained by phonon calculations in the harmonic approximation. The phonon bands dispersion curves (left column) and integrated partial DOS of atoms in equivalent site (right column) are shown. Thermodynamic properties are given in primitive cell formula: 20, 15, 10 and 40 atoms for α, β, $\beta' - C2/m$, and $\beta' - P2_1/m$, respectively.

Frequency units are in THz (1 THz = 33.356 cm^{-1}).

2.3.1 Pure element: As$-A7$, $R\bar{3}m$ (166), primitive cell: 2 atoms

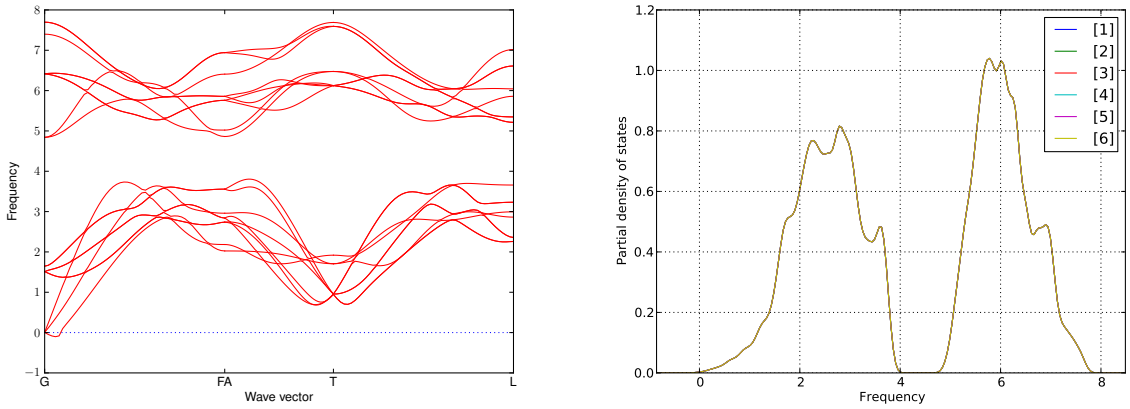

Figure S10: Phonon bands dispersion curves and integrated partial DOS of As$-A7$.

2.3.2 Pure element: Te$-A8$, $P3_121$ (152), 3 atoms

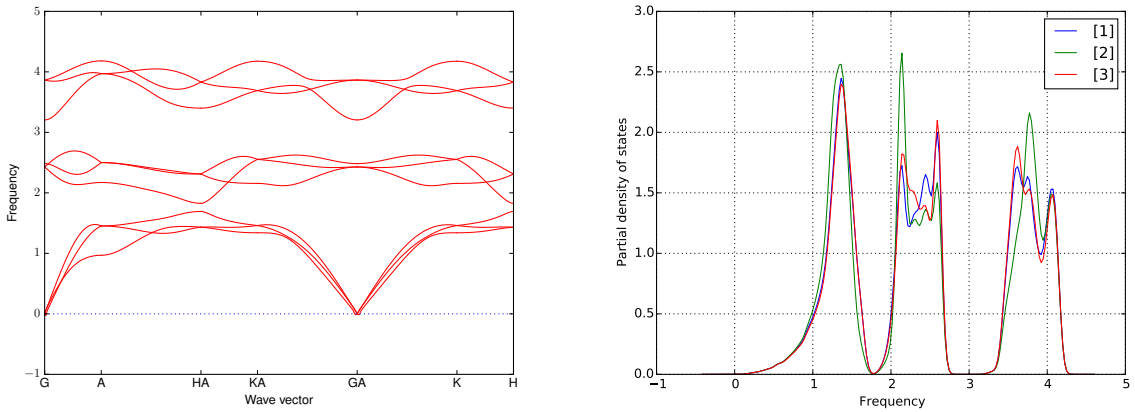

Figure S11: Phonon bands dispersion curves and integrated partial DOS of Te$-A8$.

2.3.3 $\alpha-\mathbf{As_2Te_3}$ phase, $C2/m(12)$

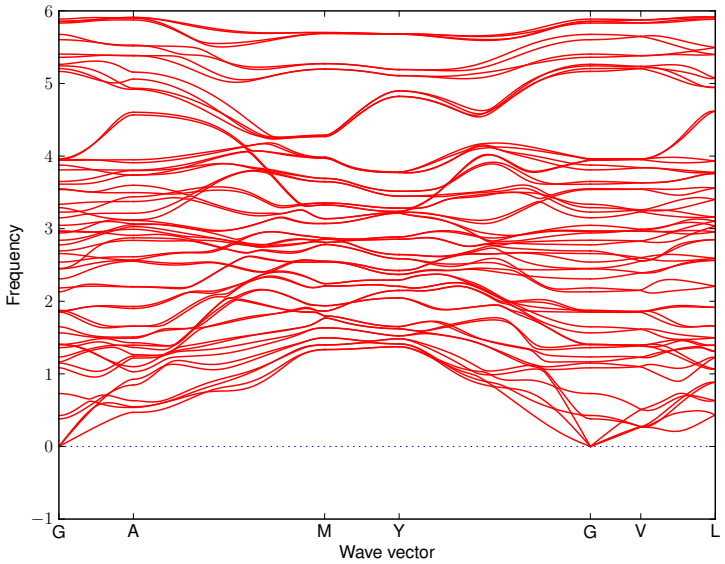

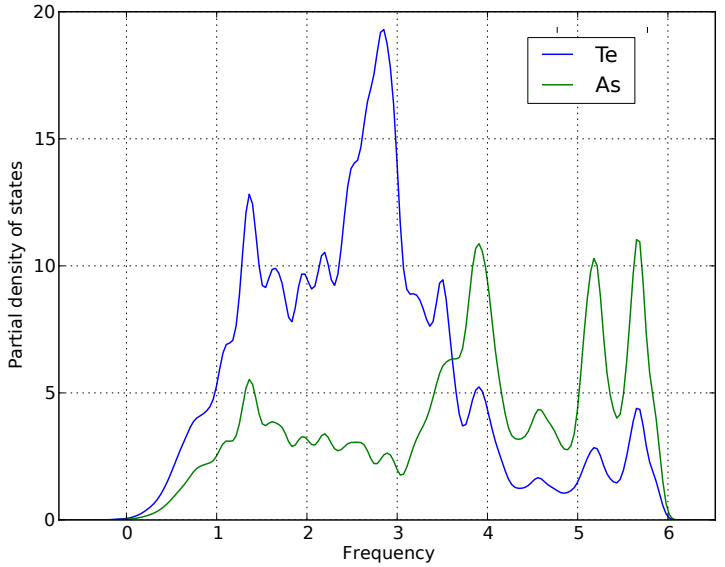

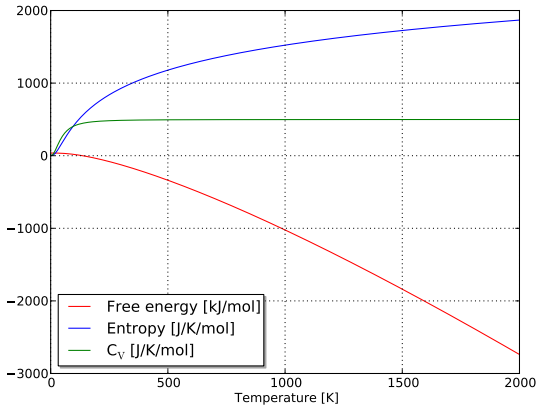

Figure S12: Phonon bands dispersion curves, integrated partial DOS and thermal properties of $\alpha-As_2Te_3$ phase.

2.3.4 $\beta-\mathbf{As_2Te_3}$ phase, $R\bar{3}m(166)$

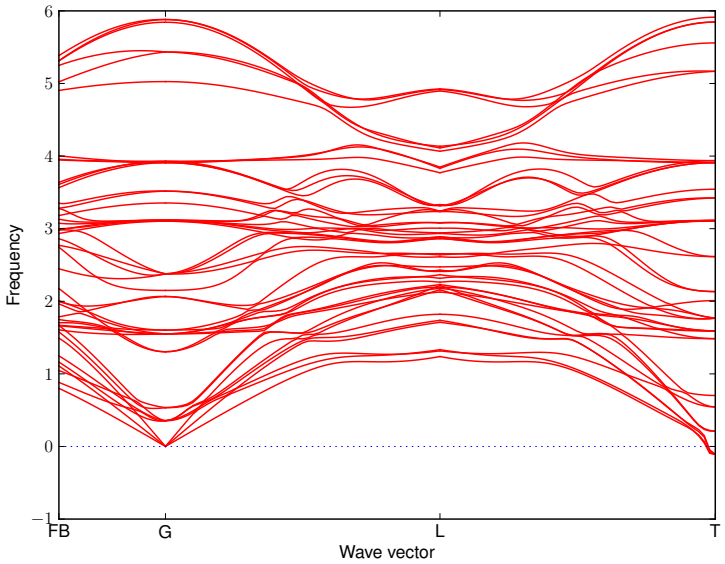

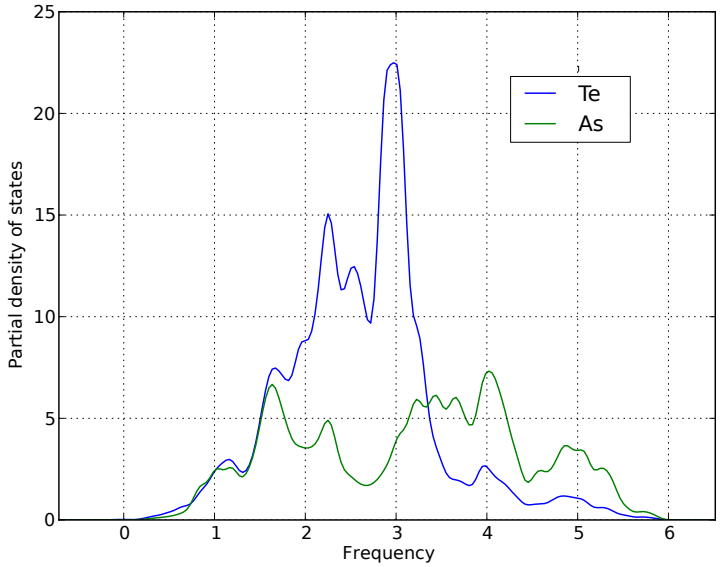

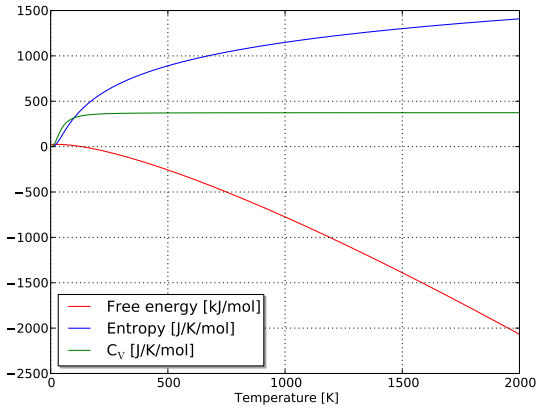

Figure S13: Phonon bands dispersion curves, integrated partial DOS and thermal properties of $\beta-As_2Te_3$ phase.

2.3.5 $\beta'-\mathbf{As_2Te_3}$ phase, $C2/m(12)$

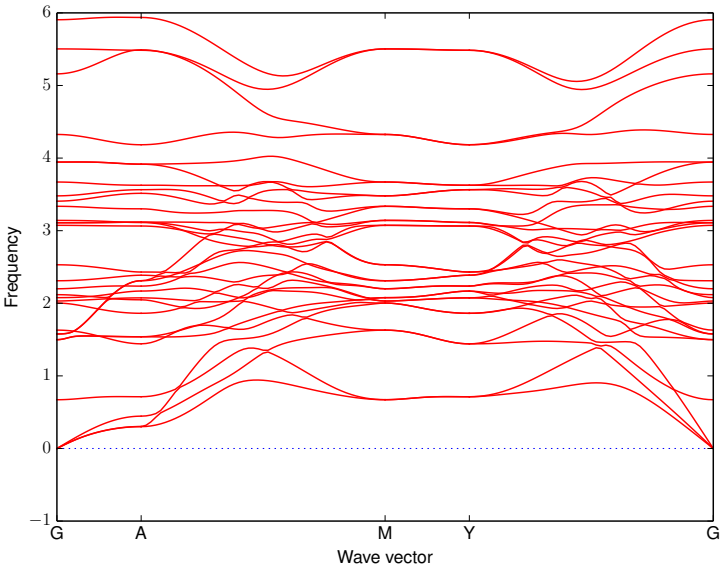

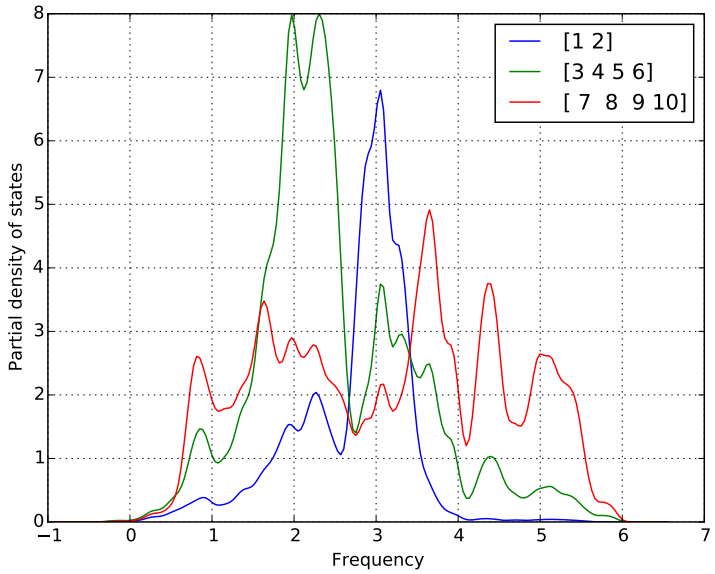

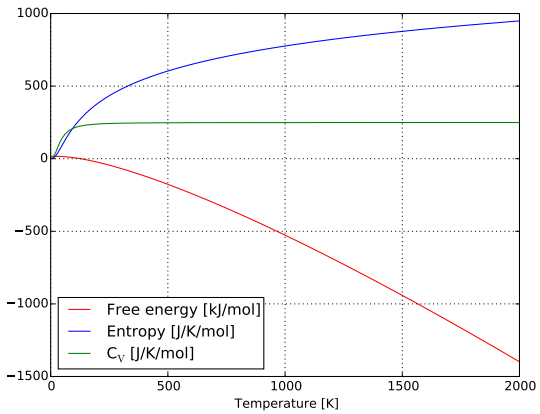

Figure S14: Phonon bands dispersion curves, integrated partial DOS and thermal properties of $\beta'-As_2Te_3$ phase, $C2/m(12)$.

2.3.6 $\beta'-As_2Te_3$ phase, $P2_1/m(11)$

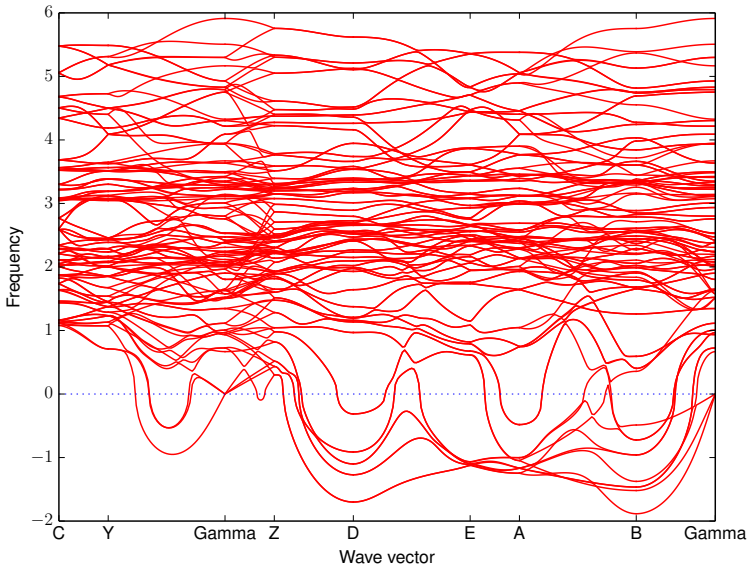

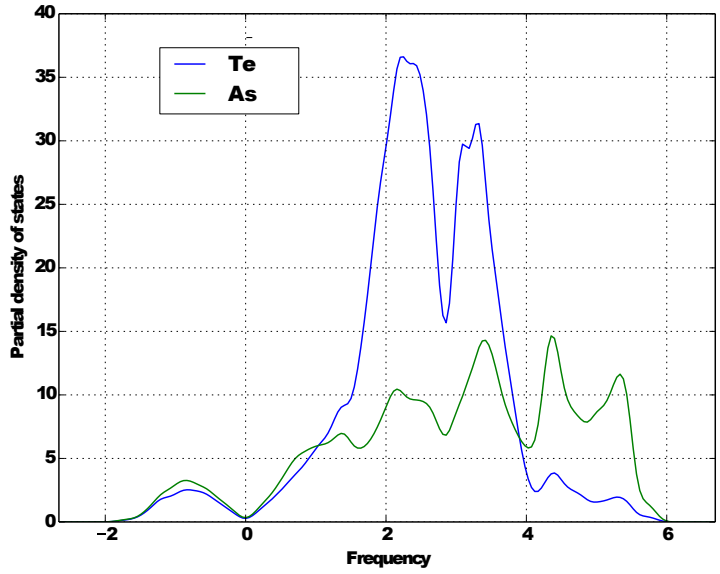

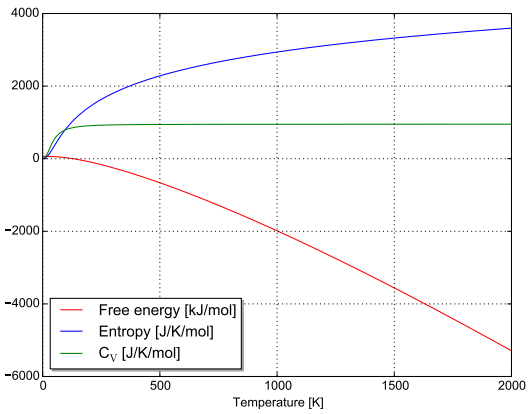

Figure S15: Phonon bands dispersion curves, integrated partial DOS and thermal properties of $\beta'-As_2Te_3$ phase, $C2/m(11)$.

2.4 Band gap as a function of an isotropic stress

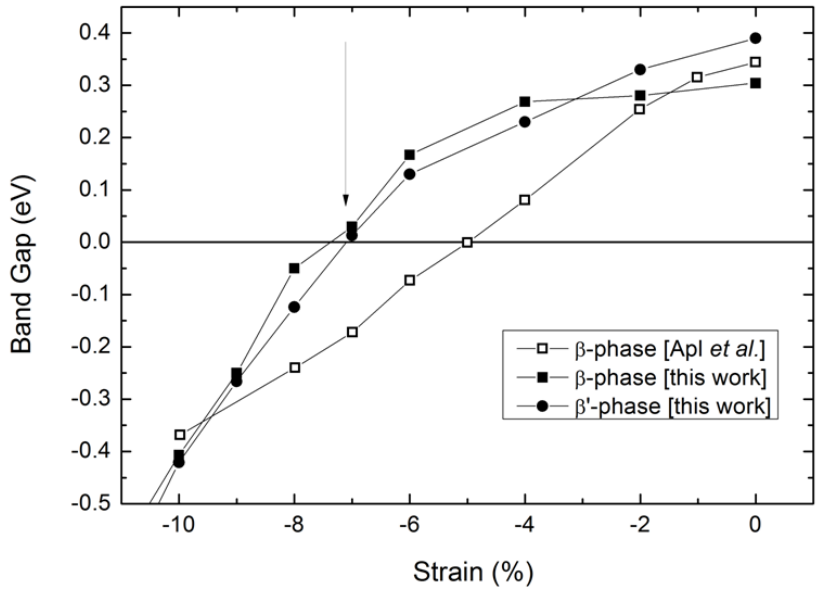

Figure S16: Electronic band gap calculated as a function of an isotropic stress of the $\beta-As_2Te_3$ and $\beta'-As_2Te_3$ phase.

The figure S16 has been obtained by the investigation of the overlapping electronic bands of As_2Te_3 at the Fermi level during an isotropic stress given, as illustrated in figure S17.

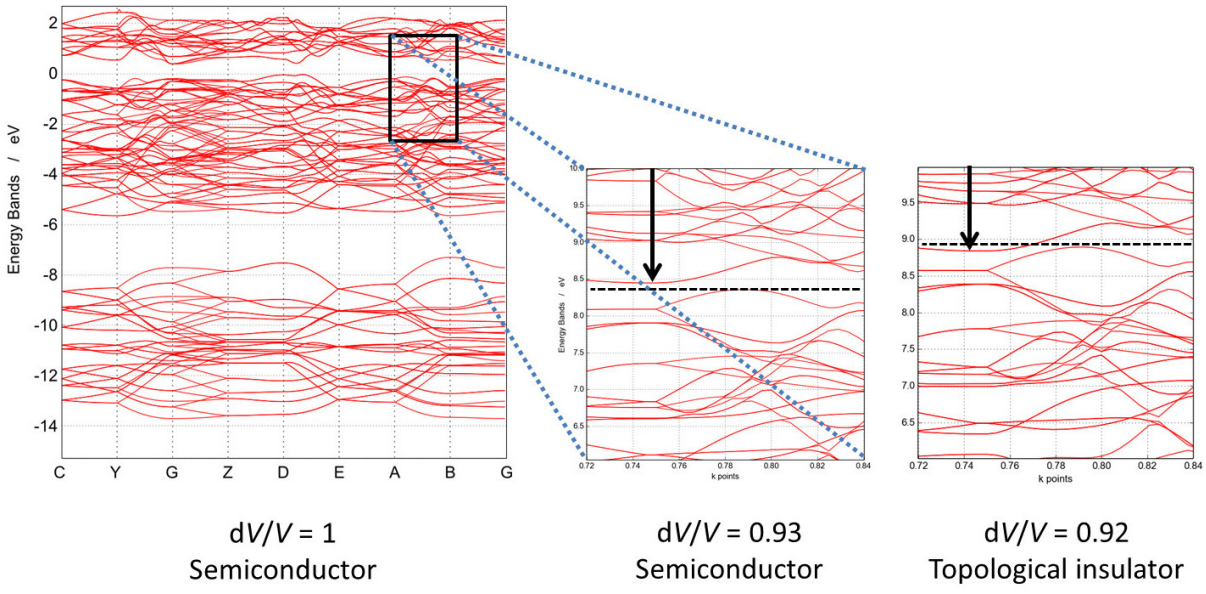

Figure S17: Zoom windows of the electronic band gap of the $\beta-As_2Te_3$ under pressure.

List of Figures